



Article

A Deep Neural Network-Assisted Approach to Enhance Short-Term Optimal Operational Scheduling of a Microgrid

Fatma Yaprakdal ^{1,*}, M. Berkay Yılmaz ², Mustafa Baysal ¹  and Amjad Anvari-Moghaddam ^{3,4} 

¹ Faculty of Electrical and Electronics Engineering, Yildiz Technical University, Davutpasa Campus, 34220 Esenler, Istanbul, Turkey; baysal@yildiz.edu.tr

² Computer Engineering Department, Akdeniz University, Antalya Campus, Dumlupinar Boulevard, 07058 Antalya, Turkey; berkayyilmaz@akdeniz.edu.tr

³ Department of Energy Technology, Aalborg University, 9220 Aalborg East, Denmark; aam@et.aau.dk

⁴ Faculty of Electrical and Computer Engineering, University of Tabriz, Tabriz 5166616471, Iran

* Correspondence: f4913026@std.yildiz.edu.tr

Received: 6 February 2020; Accepted: 14 February 2020; Published: 22 February 2020



Abstract: The inherent variability of large-scale renewable energy generation leads to significant difficulties in microgrid energy management. Likewise, the effects of human behaviors in response to the changes in electricity tariffs as well as seasons result in changes in electricity consumption. Thus, proper scheduling and planning of power system operations require accurate load demand and renewable energy generation estimation studies, especially for short-term periods (hour-ahead, day-ahead). The time-sequence variation in aggregated electrical load and bulk photovoltaic power output are considered in this study to promote the supply-demand balance in the short-term optimal operational scheduling framework of a reconfigurable microgrid by integrating the forecasting results. A bi-directional long short-term memory units based deep recurrent neural network model, DRNN Bi-LSTM, is designed to provide accurate aggregated electrical load demand and the bulk photovoltaic power generation forecasting results. The real-world data set is utilized to test the proposed forecasting model, and based on the results, the DRNN Bi-LSTM model performs better in comparison with other methods in the surveyed literature. Meanwhile, the optimal operational scheduling framework is studied by simultaneously making a day-ahead optimal reconfiguration plan and optimal dispatching of controllable distributed generation units which are considered as optimal operation solutions. A combined approach of basic and selective particle swarm optimization methods, PSO&SPSO, is utilized for that combinatorial, non-linear, non-deterministic polynomial-time-hard (NP-hard), complex optimization study by aiming minimization of the aggregated real power losses of the microgrid subject to diverse equality and inequality constraints. A reconfigurable microgrid test system that includes photovoltaic power and diesel distributed generators is used for the optimal operational scheduling framework. As a whole, this study contributes to the optimal operational scheduling of reconfigurable microgrid with electrical energy demand and renewable energy forecasting by way of the developed DRNN Bi-LSTM model. The results indicate that optimal operational scheduling of reconfigurable microgrid with deep learning assisted approach could not only reduce real power losses but also improve system in an economic way.

Keywords: day-ahead operational scheduling; reconfigurable microgrid; DRNN Bi-LSTM; aggregated load forecasting; bulk photovoltaic power generation forecasting

1. Introduction

Traditional power systems require innovation to bridge the gap between demand and supply while also overcome essential challenges such as grid reliability, grid robustness, customer electricity cost minimization, etc. Accordingly, the so-called smart grids have been developed based on the recent integration of modern communication technologies and infrastructures into conventional grids [1]. A smart grid can be defined in short as the computerization of the electrical networks with the primary objective of decreasing costs to the consumer while improving the reliability and quality of the power supply. Even though the use of computers and digital technology as part of the electrical grid has existed for at least a few decades, this technology has primarily been used for Supervisory Control and Data Acquisition (SCADA) rather than the autonomous intelligent control which is what smart grid paradigms aim for [2]. The smart grid concept is mainly comprised of microgrids (MGs) as key components [3]. These are parts of a central grid that can operate independently from the central utility grid [4,5]. A point of common coupling (PCC) is used for ensuring interactions with a central grid where the microgrid is connected to a central grid. A PCC located on the primary side of the transformer defines the separation between the central grid and the microgrid. In addition to providing local customers with their thermal and electricity needs, microgrids also improve local reliability while reducing emissions thus resulting in lower energy supply costs. Hence, microgrids are frequently utilized and accepted in the utility power industry, due mostly to their environmental and economic benefits. When the external grid suffers from disturbances or grid-connected mode, an MG system can be used in either islanded mode with the external grid supporting part of the power consumption and consisting of distributed energy resources (DERs), power conversion circuits, storage units and adjustable loads thereby providing sustainable energy solutions [6]. An MG system can be operated in either islanded mode in case the external grid suffers from disturbances or grid-connected mode, where the external grid supports part of the power consumption, and consists of distributed energy resources (DERs), power conversion circuits, storage units and adjustable loads thereby providing sustainable energy solutions [7–9]. There are a wide range of distributed generation (DG) units such as wind turbines (WTs), photovoltaics (PVs), and distributed storage (DS) units such as batteries as part of DERs [7]. Power generation in the MG system is generally utilized through the use of DERs or/and conventional power generators, such as diesel generators [10]. Power from in-plant generators has to be utilized for critical loads either to complement the grid or as an emergency source which can tolerate very little or no interruptions. The simplicity and ease of maintenance of diesel generators make them a perfect match for use under these circumstances. External supply assistance is not required to start them and they come in a wide range of ratings [11].

Additional interest has sparked recently for the use and development of renewable energy resources due to factors related to global warming and the energy crisis over the past few decades [12,13]. Minimum fuel cost has been the dominant strategy for electric power dispatching until now; however, environmental concerns have to be taken into consideration. Hereof, future demands of power grids can be supplied via microgrids that can meet these requirements [14]. A significant number of microgrid demonstration projects have been put forth in various countries including the U.S., E.U., Japan and Canada where microgrids have been integrated with the development agenda of future electric grids [15]. The penetration of microgrids has thereby increased rapidly, gradually reaching significant levels. Microgrids make up low voltage (LV) networks with distributed generation units complete with energy storage units and controllable loads (e.g. water heaters, air condition) offering considerable control capabilities over the power system operation. Extensive complications arise in the operation of an LV grid due to the operation of micro-sources in the power system, but in the meantime, it can also provide noticeable benefits to the overall network performance when managed and coordinated in an efficient manner [16]. Wind turbines and photovoltaic panels which are currently the important appliances for extracting solar energy are typical non-dispatchable DERs used in MGs for overcoming issues related to alternative, sustainable, and clean energy [10,17]. Solar energy is considered among the most promising renewable resources for bulk power generation in addition to

being an infinite, eco-friendly form of Energy. Nonetheless, it is highly dependent on temperature and solar radiation, which have direct effects on the solar power output thus resulting in the intermittent and variable characteristic of solar power [18]. Another dimension of uncertainty is present in the load forecast with the adoption of renewable distributed generation technologies [19]. Forecast needs are underlined by the presence of a de-regulated environment, especially for distribution networks. Load forecasting is essential for the convenient operation of the electrical industry [20]. Reliable short-term (hour-ahead, day-ahead) load forecasts under service constraints are required for actions such as network management, load dispatch, and network reconfiguration. Short-term load forecasting algorithms are among methodologies that aim to increase the effectiveness of planning, operation, and conduction in electric energy systems [21–25].

Network reconfiguration that is considered as a significant solution for microgrids has been used for optimal operation management. It can be defined as operational schemes that alter the network topology by modifying the on/off status of remotely controlled sectionalizing switches (normally closed switches) and tie switches (normally open switches) of active distribution networks thereby enabling the controlling of power flow from substation to power consumers with additional benefits such as load balancing, real power loss reducing, optimizing the load sharing between parallel circuits by directing power flow along contractual paths [26]. However, the majority of the network reconfiguration (NR) studies aim to decrease power losses on the grids [27]. Real power losses in active distribution networks can be decreased by way of two essential methods: the NR and the optimal dispatch (OD) of diesel DG units. The NR technique can only partially mitigate the losses due to the distribution systems. The OD of DGs is a significant contributor to obtain greater power loss reduction [28]. The sizing of DGs and NR has been implemented in [29–31] either sequentially or simultaneously to attain further reductions in power loss. Optimal NR and distributed generation allocation have been carried out simultaneously in the distribution network. Nonetheless, in [28] it has been observed that significant improvements such as voltage profile improvement and reduced energy production cost in the entire system can be attained via the simultaneous application of NR and OD of the DGs techniques during the analysis. Moreover, the proposed joint approach of the PSO and SPSO methods displayed a higher performance in power loss reduction in comparison with the other methods in the literature [29–32].

The optimal operational scheduling problem should be resolved for attaining the minimum loss under the new profile if the net load profile keeps changing. The net load profile is calculated as a sum of electrical power consumption and renewable power generation for each period. Therefore, the dynamic NR and dispatch of diesel DGs can be pre-performed in response to load and renewable power output changes with the forecasted electrical power consumption and renewable power generation profiles [33]. Various articles have been published in the literature on the scope of general power system operational scheduling and planning. However, load and renewable power generation output estimates have been used in very few. In [33], the data-driven NR based on the 1-h-ahead load forecasting is solved in a dynamic and pre-event manner with the utilization of support vector regression (SVR) and parallel parameters optimization based on short-term load forecasting results as an input to the reconfiguration algorithm. An SVR-based short-term load forecasting approach is used in [34] to cooperate with the NR for minimizing the system loss. These papers only consider NR within the operational planning studies and machine learning-based 1-h-ahead load forecasting results are utilized as input to the optimization frameworks. Since the next days' power generation must be scheduled every day in power systems, a day-ahead short-term load forecasting is an obligatory daily task for power dispatch. The economic operation and reliability of the system are significantly affected by its accuracy. An artificial neural network-based method for forecasting the next day's load as well as the economic scheduling for that particular load is put forth in [35]. The economic dispatch problem integrated with artificial neural network-based short-term load forecasting is taken into consideration in [36] regarding studies on operational scheduling with power dispatch. Reference [37] contributes to the optimal load dispatch of a community MG with deep learning-based solar power and load forecasting. A two-stage dispatch model based on the day-ahead scheduling and real-time scheduling to optimize the dispatch

of MGs is presented in [38]. A two-phase approach for short-term optimal scheduling operation integrating intermittent renewable energy sources for sustainable energy consumption is proposed in [39]. A day-ahead energy acquisition model is developed in the first phase while the second phase presents real-time scheduling coordination with hourly NR. Reference [40] puts forth a method for optimal scheduling and operation of load aggregators with electric energy storage in power markets to schedule the imported power in each period of the next day with day-ahead forecasted price and load. However, it has been observed upon examining the power system operational scheduling and planning studies that the simultaneous approach of NR and OD of DG units has not been performed as in [28]. Moreover, one of the studies in the literature has made use of DL-based load and solar power forecasting results and it is concluded that the proposed LSTM-based deep RNN model has a great potential for more accurate short-term forecasting results to promote economic power dispatch on a microgrid as an optimal operational work [37]. The results of this study have encouraged us in terms of microgrid optimal operational studies. Therefore, the present study is supported by DL-based prediction studies and is put forth as a continuation of the study in [28]. Furthermore, DRNN-LSTM is mostly used among the deep learning approaches for short-term and aggregated level forecasting studies as can be seen in [37,41–44]. Here, A DRNN model based on Bi-LSTM units has been developed as a significant contribution of this study to forecast the aggregated electrical power load and bulk PV power output of reconfigurable MG during a short-term period and the net load profile is considered as a sum of demand consumption and PV power generation for each hour in a day.

The rest of the study is organized as follows: Section 2 provides a detailed description of the DRNN Bi-LSTM model for forecasting aggregated power load and PV power output and the optimization model for determining the optimal day-ahead operational scheduling of the reconfigurable MG. The simulation results and discussions are given in Section 3 while the conclusions are presented in Section 3.

2. The Architecture of the Proposed Approach

It is of significant importance with regard to developing economies to put into practice power system operational planning practices for employing the already existing capacity in the best possible manner [45]. Optimal generation scheduling is especially important for microgrid operation [46]. As such, putting forth the least-cost dispatch among the DGs that minimize the total operating cost, while meeting the electrical load and satisfying various technical, environmental, and operating constraints is part of the daily operation of a microgrid [47]. Contrarily, real load data measured at that instant in a conventional dynamic power system reconfiguration work is used for putting forth the optimal topology at each scheduled time point. An accurate prediction of the load power is possible by way of the development of load forecasting technique which takes place at a future time and provides more information on load changes. Optimal topology with the incorporation of load forecasting can be resolved subject to forecasted load conditions during a longer time period rather than the use of a snapshot of the energy consumption at the time when the reconfiguration actualizes; thereby, this information can be used by the distribution network operator for an improved system reconfiguration operation as well as for bringing about the desired optimal solutions [33]. Moreover, it is possible to operate the smart grids in an economical manner only via accurate forecasting of solar power/irradiance [12].

In this context, this study develops a DRNN Bi-LSTM model to forecast hourly power load and the hourly PV power output over a short-term horizon (24-h) respectively. Afterwards, the optimal operational scheduling model of the reconfigurable MG which contains aggregated power load, bulk PV arrays, and diesel DGS is established under different scenarios. In the optimal operational scheduling model, the aggregated load and the PV power output are obtained from the estimation results of the DRNN Bi-LSTM model [37].

2.1. Day-Ahead Load and Solar Power Output Forecasting

These forecasting studies are generally carried out at aggregated and individual levels and are classified based on the forecasting horizons as follows:

- Very Short-Term Load Forecasting (VSTLF): ranging from seconds or minutes to several hours [48],
- Short-Term Load Forecasting (STLF): ranging from hours to weeks [49],
- Medium and Long-Term Load Forecasting (MTLF/ LTLF): ranging from months to years [50].

It is critical for power companies to put forth an accurate forecast of load profile for the next 24 h as it can have a direct impact on the optimal hourly scheduling of the generation units in addition to their participation in different energy markets. Interestingly, the number of values to predict can also be used for classifying the forecasting models. There are two main groups: the first group consists of those that forecast only one value (next hour's value, next day's peak value, next day's total value, etc.); the second group is comprised of forecasts with multiple values, such as next hours or even next day's hourly forecast. Single-value forecasts are used for on-line operation and optimization of load flows, whereas multiple-value forecasts are utilized for generator scheduling and economic dispatching. Energy demand forecasting has been an important field in order to allow generation planning and adaptation. In addition to demand forecasting, electrical generation forecasting models have also attracted increased attention recently, especially with regard to renewable generation sources that depend on the forecasting of a particular energy resource (solar radiation, wind, etc.) [50].

Forecasts, usually 24-h ahead, should be used for anticipating the electricity demand to be met with sufficient energy and thus it will be apparent whether it is necessary to buy energy in the market (energy defect) or sell it (excess energy). This is known as STLF which helps in planning the operation of generators and energy-related systems owned by the utility [51]. In the meantime, there are many factors such as calendar type, weather, climate, and special activity that have an impact on load consumption. Similarly, the majority of the forecasting approaches applied for power forecasting are available for load forecasting solutions [10]. Load forecasting is essentially a time series forecasting problem. Autoregressive moving averages models [52], auto-regressive integrated moving average [53], linear regression (LR) [54], iteratively re-weighted least-squares (IRWLS) [55]; nonlinear methods such as artificial neural network [56], multi-layer perceptron (MLP) [57], regression decision tree machine learning algorithm [58], general regression neural network and support vector machine (SVM) [59] have recently been utilized for this kind of forecasting study. However, deep neural networks (DNNs), a type of artificial neural networks (ANN) with multiple hidden layers of neurons between the input and output [8], have recently been increasing in popularity as the latest developed subset of machine learning techniques for time series electrical load forecasting problems [60]. The short-term and aggregated level has the highest number of studies on electrical load estimation with LSTM-RNN as the most commonly used deep learning method in these studies.

PV panels are used on-grid or off-grid to provide electricity to individual buildings, aggregated settlements, and commercial and industrial areas. The intermittent nature of solar energy makes it very difficult to establish a balance between electricity generation and consumption. The successful integration of solar energy into the power grid requires an accurate PV power prediction thereby reducing the impact of the uncertainty of output power of PV panels leading to a more stable system [61]. Power forecasting for PV power generation has especially become one of the fundamental technologies for improving the quality of operational scheduling and reducing spare capacity reserves [62]. The methods used to estimate the PV generation which is influenced by atmospheric conditions such as temperature, cloud amount, dust and relative humidity are generally divided into three main categories; time-series statistical methods, physical methods, and combined methods. Nonetheless, solar forecasting studies frequently utilize artificial intelligence (AI) techniques due to their capacity to solve complex and nonlinear data structures. Deep learning algorithms have especially been used in solar power prediction studies that outperform traditional methods as a sub-branch of AI methods.

The most widely used deep learning method is deep LSTM-RNN [44] and the combination of LSTM with other DL algorithms [63,64].

2.1.1. Forecasting Model

DNN is broadly accepted to model complex non-linear systems in engineering. Besides, the computation of DNN only includes basic algebraic equations, thus providing a fast computation speed [8]. Recent forecasting studies have put forth that improved accuracies are attained by DL systems in comparison with conventional methods. CNN is a type of feed-forward artificial neural network in the field of machine learning research where a structure is formed among artificial neurons inspired by the organization of human neurons [65]. CNN is most utilized in cases related to tasks in which data have high local correlation such as visual imagery, video prediction, and text categorization. It can capture when the same pattern appears in different regions [66]. A CNN architecture consists of a stack of distinct layers that transform the input data into an output volume. The network structure of the CNN model is comprised of distinct types of layers such as convolution layers and pooling layers [65]. In addition, CNNs require multi-dimensional inputs to attain a high prediction accuracy. Time series data, e.g., the energy consumption data, forecasting poses a significant challenge even for deep learning technologies when the desired output is another time series, namely the 24 h of the next day. Contrary to such traditional feed-forward networks (FFNs) where all inputs and outputs are assumed to be independent of each other, RNN maintains a memory about the history of all past inputs using the internal state. RNN contains feedback connections to ensure the flow of activations in a loop. RNN can be considered more like a human brain because of the recurrent connectivity found in the visual cortex of the brain. Therefore, an RNN architecture is more appropriate for time series, as the case of the present work. It proposes an RNN consisting of a Bi-LSTM unit to learn the sequential flow of various measurements through consecutive days and hours, predicting electrical energy consumption and bulk PV power generation values through the next 24 h at an aggregated level for day-ahead operational scheduling of reconfigurable MG. Information flow is multidirectional with the Bi-LSTM unit.

All hyper-parameters (number of layers, number of hidden units, length of input feature sequence, etc . . .) are chosen according to the tests applied during the dates of 08.01.2016–31.12.2016, with models trained on a small subset of the previous samples. A few experiments have been conducted for that purpose, without fine-tuning of the hyper-parameters.

The proposed RNN consists of a sequence input layer of size 11 (one sequence input for each feature), followed by a Bi-LSTM layer of 150 hidden units, a fully connected layer that outputs a single sequence of either PV power generation or electrical demand, and finalized by a regression layer. Adam optimizer was used and the training was stopped earlier to prevent overfitting to training data. The initial learning rate is 0.005.

The test data used represents electrical energy consumption and PV power generation measurements, along with a number of other observations in the Czech Republic from 01.01.2012 to 31.12.2016. There are 24 measurements per day with 1-h resolution. 5-fold cross-validation is applied over the entire dataset to train and test (training on the first 4 years and testing on the 5th year, training on first 3 plus the last year and testing on 4th year, etc . . .).

Two different models are trained to forecast daily PV power generation and electrical demand values separately. The input features for daily power load forecasting model are previous 6 days' (hourly) month, day, hour, PV power generation, electrical energy consumption with pumping load, electrical energy consumption, wind speed, temperature, direct horizontal radiation, diffusion horizontal radiation; while these features are previous 6 days' (hourly) month, day, hour, PV power generation, wind speed, temperature, direct horizontal radiation, diffusion horizontal radiation for daily PV power generation forecasting model. Each feature input is a sequence (past 6 days) of length $24 \times 6 = 144$. RNN outputs either a sequence of forecasted PVPP or forecasted load values. The

proposed RNN is shown in Figure 1. All available input features are used without any handcrafted modification or selection, to allow the deep model to capture all necessary information from raw data.

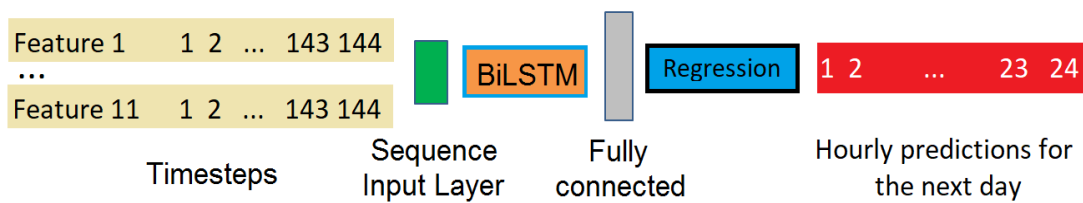


Figure 1. The proposed RNN model.

During training and testing, only the feature sequences starting just at the start of a new day at time 00:00 are considered. During training, it is also possible to use intermediate sequences (such as previous 144 hours' at time 14:00 as input, with a corresponding ground truth output sequence for the next 24 h until next day's 14:00) however, such intermediate sequences are skipped for simplicity.

As an example; when the first-ever year in the dataset (2012) is used in training, input time-steps for the first-ever training sample will thus be the first 6 days' (from 01.01.2012 to 06.01.2012) hourly feature measurements (of length 144 for each feature), with the target as either the hourly electrical demand or PVPP values for 07.01.2012.

To normalize the data; month, day and hour are divided by their maximum values plus one, i.e., 13 for the month, 32 for day and 25 for the hour. With the help of this normalization; maximum values become just less than one, easier to converge to with most activation functions. Other features are normalized by subtracting their mean and dividing to their standard deviation so that these features become zero mean and unit variance. Let x_i be some observation of feature type x (Can be wind power plant (WPP) generation, PVPP, electrical load consumption with pumping, electrical load consumption, wind speed, temperature, direct horizontal radiation or diffusion horizontal radiation). x_i is normalized as:

$$x_i^n = (x_i - \mu(x)) / \sigma(x) \quad (1)$$

$\mu(x)$ and $\sigma(x)$ are calculated from the complete dataset. Performances (root mean square error (RMSE)) of the proposed RNNs during the learning phase for power demand and PV power generation with the number of training iterations are shown in Figures 2 and 3 accordingly, trained with the first 80% of the days (first 4 years).

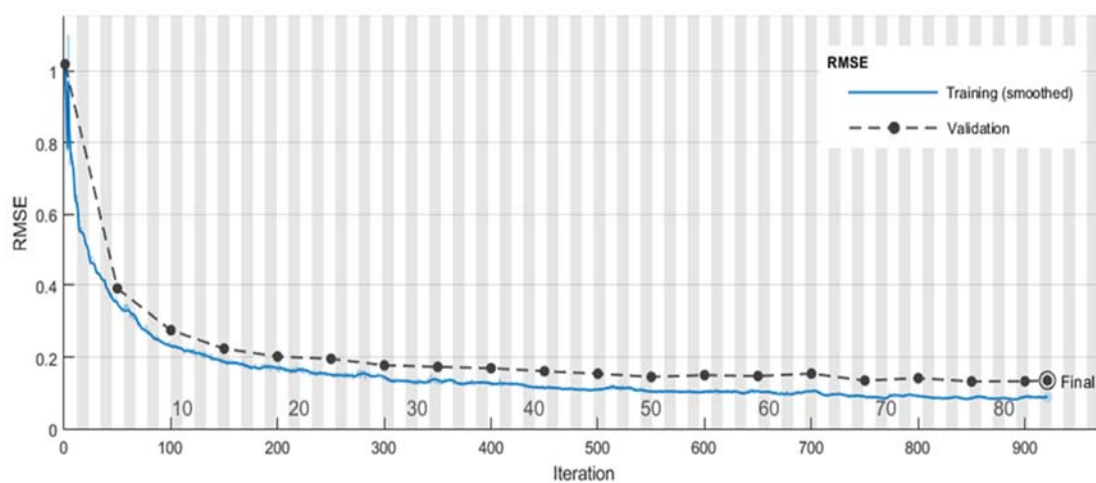


Figure 2. Performance (RMSE) of the proposed RNN during the learning phase for power demand, trained with the first 80% of the days (first 4 years).

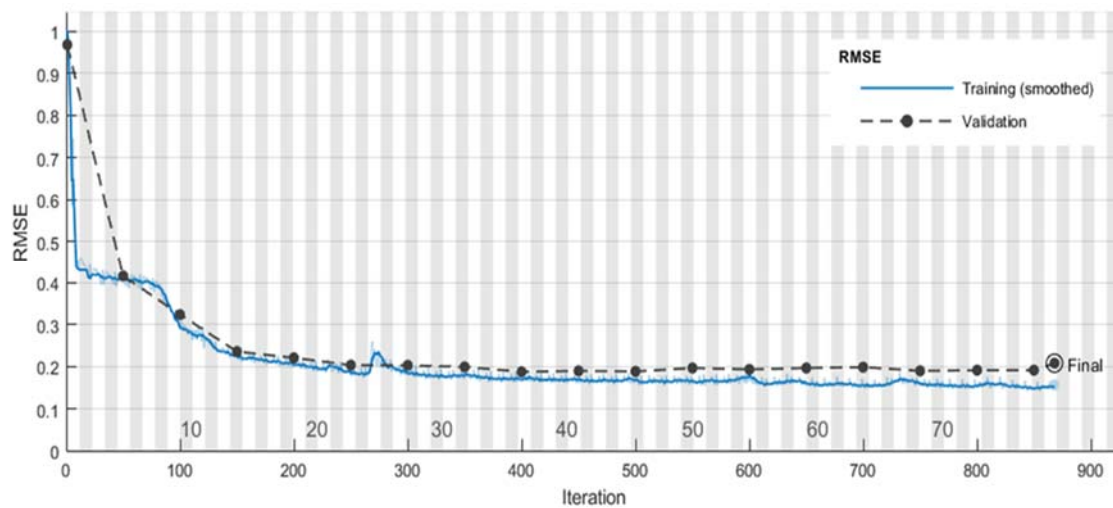


Figure 3. Performance (RMSE) of the proposed RNN during the learning phase for PV power generation, trained with the first 80% of the days (first 4 years).

2.1.2. Baseline Feed-Forward Neural Network

RNNs have significantly stronger abilities in modelling complex processes and learning temporal behaviors rather than a normal feedforward network [67]. However, a feed-forward neural network (FFNN) which accepts inputs of feature hour sequences all stacked as a single 1D feature vector (length $11 \times 144 = 1584$) and outputs 24 hourly forecasts for the following day is utilized for comparison here. There are 12 hidden units in the hidden layer, chosen on a small validation set similar to that of the RNN. The baseline FFNN model is shown in Figure 4.

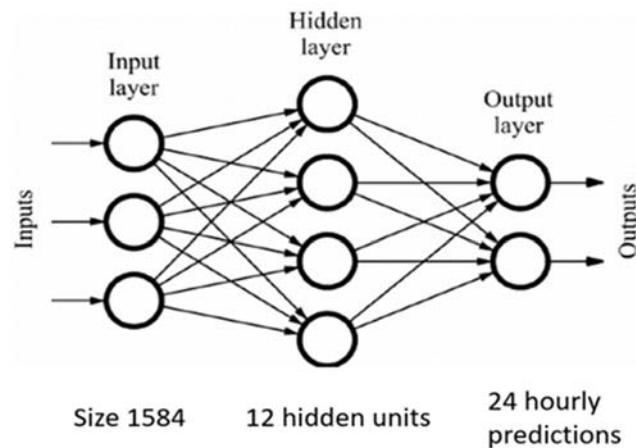


Figure 4. The baseline FFNN model.

2.1.3. Error Metrics

In the following equation:

$$e_j = a_j - p_j \quad (2)$$

is the error. Several error metrics are reported in this study for comparison.

- Scale-dependent measures:

Mean absolute error (MAE) is formulated as:

$$MAE = \frac{1}{n} \sum_{j=1}^n |e_j|, 0 \leq MAE < \infty \quad (3)$$

and MAE is easy to interpret and heavily used in regression and time-series problems.

Root mean square error (RMSE) is defined as:

$$RMSE = \sqrt{\frac{1}{n} \sum_{j=1}^n e_j^2}, 0 \leq RMSE < \infty \quad (4)$$

and RMSE is a quadratic error metric, representing the standard deviation of errors. RMSE exaggerates bigger errors, being more sensitive to outliers than MAE.

- Measures based on percentage errors:

Percentage errors are mostly used to compare forecast performance across several data sets as they are scale-independent. Mean absolute percentage error (MAPE) is defined as:

$$MAPE = \frac{100}{n} \sum_{j=1}^n \frac{|e_j|}{|a_j|} \quad (5)$$

and MAPE is frequently used in regression and time-series problems to measure the accuracy of predictions [68]. If there are zero values in the data, MAPE cannot be calculated. Similarly, MAPE values become large if there are small values in the data. There is no upper limit on the MAPE value. MAPE values are biased in the sense that they systematically reward the method that is predicting smaller values.

Symmetric mean absolute percentage error (sMAPE) is defined as:

$$sMAPE = \frac{100}{n} \sum_{j=1}^n \frac{2|e_j|}{|a_j| + |p_j|} \quad (6)$$

and sMAPE is an alternative to MAPE if there are data points at zero or close to zero. Such problems can be less severe for sMAPE. sMAPE may still involve division by a number close to zero.

Large (or infinite) errors can be avoided by excluding the non-positive data or that of less than one [65]. However, this solution is ad hoc and is impossible to apply in practical applications. Moreover, it leads to the problem of how outliers can be removed. The exclusion of outliers may result in the loss of information when the data involve numerous small a_j 's.

Because the underlying error distributions of percentage errors have only positive values and no upper bound, percentage errors are highly prone to right-skewed asymmetry in practice [68]. Percentage errors are neither resistant nor robust measures because a few outliers can dominate and they will not be close in value for many distributions. This work proposes to get rid of the undefined percentage errors by adding a constant positive number α to each data point a_j and prediction p_j so that all data points are positive and much greater than zero. MAPE and sMAPE thus use $a_j + \alpha$. and $p_j + \alpha$ values in the corresponding formulas. It is further proposed that scale-dependent measures better represent the magnitude of the error than percentage errors when the data is normalized to be unit variance and zero mean.

Both the errors on normalized and unnormalized actual values $a_j^n \sigma(x) + \mu(x)$ and predictions $p_j^n \sigma(x) + \mu(x)$ are reported. In some sense, the proposed process of adding a fixed constant is inevitable as for the unnormalized data the following MAPE value is calculated:

$$MAPE = \frac{100}{n} \sum_{j=1}^n \frac{|a_j^n \sigma(x) + \mu(x) - (p_j^n \sigma(x) + \mu(x))|}{|a_j^n \sigma(x) + \mu(x)|} \quad (7)$$

Simplifying to:

$$MAPE = \frac{100}{n} \sum_{j=1}^n \frac{|e_j|}{|a_j^n + \mu(x) / \sigma(x)|} \quad (8)$$

leads to smaller MAPE values as shown in the results. sMAPE is similarly affected when unnormalized data is used.

Mean absolute scaled error (MASE) is the mean absolute error of the forecast values, divided by the mean absolute error of the one-step naive forecast of training data. MASE is scale-invariant and it has predictable behaviour even when the data values are close to 0. In this work we calculate the naive forecast as the value at the same hour of the previous day, utilizing the seasonal time series formula:

$$MASE = \frac{MAE}{\frac{1}{T-24} \sum_{t=25}^T |Y_t - Y_{t-24}|} \quad (9)$$

where MAE is calculated according to Equation (3).

2.2. Optimal Operational Scheduling Problem

This section of the study focuses on the optimal operational scheduling problem of reconfigurable MGs in which the optimal radial topology of the balanced medium-voltage reconfigurable MG system as well as the optimum power generation level of diesel DGs has to be determined by the system operator to minimize real power losses. The aforementioned non-linear combinatorial problem which can be considered as a single-objective optimization problem is represented by the mathematical formulation given below [69]:

$$x = [x_1, x_2, \dots, x_{dv}] \quad (10)$$

$$\min(f_1(x), f_2(x), \dots, f_N(x)) \quad (11)$$

$$s.t. h_i(x) = 0; i = 1, \dots, p \quad (12)$$

$$g_i(x) \leq 0; i = 1, \dots, q \quad (13)$$

In this paper, the optimization problem is a minimization problem with its equality and inequality constraints given in the following sections.

• Objective Function

Power loss reduction and voltage profile improvement for the whole system are significantly influenced by NR techniques as well as OD of DG units which eventually determine the direction of power flow in an MG. Therefore, the main objective of our specific problem is the minimization of the sum of active power losses in all branches as given in the following equation [28]:

$$\min \left\{ P_L = \sum_{i=1}^b |I_i|^2 R_i \right\} \quad (14)$$

• Equality and Inequality Constraints

Various equality and inequality constraints of the reconfigurable MG have to be taken into consideration during the simultaneous application of NR and OD of DGs in reconfigurable MG. The following constraints have been considered for this study:

(1) Equality Constraint

Power balance constraint has to be met based on the following equation:

$$P_{EP} + \sum_{j=1}^{N_{DG}} P_{DGj} - \sum_{i=1}^{N_{MGL}} P_{MGLi} - P_L = 0 \quad (15)$$

(2) Inequality Constraints

The constraint for the maximum and minimum active power generation of dispatchable units can be represented as given below:

$$P_{DGi}^{min}(t) \leq P_{DGi}(t) \leq P_{DGi}^{max}(t) \quad (16)$$

The amount of the flowing current I_i at the i^{th} branch should not exceed its maximum thermal value I_i^{max} [28]:

$$|I_i| \leq I_i^{max} \quad (17)$$

The bus voltage values, V_i , should vary between the minimum and maximum values after reconfiguration and slack bus voltage is taken as following [70]. The limits in the present study have been set to $V_{min} = 0.90$ p.u. and $V_{max} = 1.10$ p.u., respectively:

$$V_{min} \leq V_i \leq V_{max}; V_{slack} = 1 \quad (18)$$

• Radiality Constraint

All possible MG configurations have to be in radial condition throughout the NR process. Moreover, there must not be any loops and all loads must be connected to the main power supply in the topological structure of MG which can be expressed using the following formula [28]:

$$\sum_b^{N_b} \beta_b = m - N_{sub} \quad (19)$$

• Operational Cost Calculation

Total of purchasing power cost from the main grid and the production cost of dispatchable diesel DGs is considered as the total operational cost here in this study:

$$TotalCost = Cost_{MG} + Cost_{DG} \quad (20)$$

In case it is not possible to meet the total energy demand via distributed DGs, reconfigurable MG has to purchase power from the upstream grid. The following formula is used total active power purchase for this case is calculated [71]:

$$Cost_{MG} = \sum_{t=1}^{24} v^b(t) P^b(t) \quad (21)$$

The mathematical relation given below is used for calculating the generation cost of diesel DGs on a daily basis which is comprised of the fuel cost [72].

$$Cost_{DG} = \sum_{t=1}^{24} a + b \times P_{DG}(t) + c \times (P_{DG}(t))^2 \quad (22)$$

2.2.1. Overview of PSO and SPSO

The majority of the researchers have used Particle Swarm Optimization (PSO) for solving optimization related problems in power systems. The behavior of clustered social animals such as fish and birds are used for creating the PSO method. Birds or fish move towards food at certain speeds or positions. Each particle part of the population of n particles in D -dimensional space represents a possible solution for PSO defined by two parameters as position (p) and velocity (v) that are initially chosen randomly. The movement of population members will depend on their own experience and experience from other 'friends' in the group P_{best} and G_{best} . The parameters are updated based on the following model:

$$v_{iD}^{k+1} = \omega \times v_{iD}^k + c_1 \times rand \times (p_{best-i} - x_i^k) + c_2 \times rand \times (g_{best-i} - x_i^k) \quad (23)$$

$$x_i^{k+1} = x_i^k \times v_i^{k+1} \quad (24)$$

and here, ω is calculated by the following formula:

$$\omega = \omega_{max} - (\omega_{max} - \omega_{min}) \times \left(\frac{k}{k_{max}} \right) \quad (25)$$

The velocities are confined in the range of $[0,1]$ via sigmoid transformation on the velocity parameters in binary PSO, thus ensuring that the particle position values are either 0 or 1:

$$sig(v_{iD}^{k+1}) = \frac{1}{1 + \exp(-v_{iD}^{k+1})} \quad (26)$$

$$x_{iD}^{k+1} = \begin{cases} 1, & \text{if } \sigma < sig(v_{iD}^{k+1}) \\ 0, & \text{if } \sigma \geq sig(v_{iD}^{k+1}) \end{cases} \quad (27)$$

Khalil and Gorpinich suggested a minor change to binary PSO, SPSO by keeping the search in the selected search space. The search space in SPSO at each D dimension $SD = [SD1, SD2, \dots, SDN]$ is comprised of a set of DN positions where DN represents the number of selected positions in dimension D . A fitness function is described in SPSO as is the case for the basic PSO; which maps at each D dimension from DN positions of the selective space SD leading to alter the position of each particle from being in real-valued space to be a point in the selective space, thereby changing the sigmoid transformation as per (20):

$$v_{iD}^{k+1} = \begin{cases} rand \times v_{iD}^{k+1}, & \text{if } |v_{iD}^{k+1}| < |v_{iD}^k| \\ v_{iD}^{k+1}, & \text{otherwise} \end{cases} \quad (28)$$

The number of tie switches in the MG indicates the dimension of the reconfiguration problem. When all tie switches are closed some loops are present in the network with the number of loops equal to the number of switches. All branches in the loop that define the dimension make up the search space in a certain dimension. The optimization algorithm does not take into account the branches out of any loop. The common branch that belongs to more than one loop should be placed in just one loop in the dimension. The optimum configuration can be determined via SPSO following the determination of the dimensions and search space for each dimension [28].

2.2.2. PSO&SPSO Method

The framework discussed in this study is NR in parallel with OD of DGs with an objective of minimizing real power losses with some constraints on the MG. The PSO algorithm has been selected for solving the problem due to its improved potential in the solution of discrete, nonlinear and complex optimization problems. The fact that PSO and SPSO algorithms combine the advantages of both PSO approaches can be considered as the motivation for their selection.

There are many equality and inequality constraints for the non-linear optimization problem of OD which puts forth the optimal power output of DGs to meet the estimated electrical consumptions from an economic perspective. Traditional optimization algorithms may not be sufficient for solving such problems due to local optimum solution convergence, while metaheuristic optimization algorithms, and specially PSO, have succeeded unusually in solving such types of OD problems during the last decades.

MG reconfiguration comprises the combinational part of the whole optimization problem. To attain the suitable arrangement of power and radial configuration for every load, distribution system planners operate with numerous switches. The sectionalizing switches (which are normally closed) along with the tie switches (which are normally open) to maintain radiality. An accurate switching operation plan can be attained through the various switch. The combinatorial nature of the constrained optimization problem can be easily overcome by embedding selective operators into the standard PSO.

The optimization problem turns out to be even more complex when time-sequence variation in load, power market price and output power of DGs are considered. High computation time for larger systems hindering real-time operation can be indicated as a problem for the majority of meta-heuristic methods. Hence, PSO is preferred to overcome the complexity of the optimization problem due to its faster convergence rate, accuracy, parallel calculation, and ease of application.

It is of significant importance to associate the MG parameters with optimization parameters for the simultaneous MG reconfiguration and OD problem. Two decision variable sets make up the particles in the proposed PSO&SPSO. The dimension of search space equals the number of diesel DGs regarding the OD part while it is equal to the number of tie switches in the MG about the NR part throughout the combined algorithm. This method is used for carrying out the OD for the DG units via the basic PSO, while switch positions are determined by applying the SPSO method simultaneously at every iteration [28].

2.3. The Test System Features

The standard 33-bus test system is taken into consideration as a reconfigurable MG in the present study by integrating three diesel DGs and a bulk PV generation unit as can be seen in Figure 5. The detailed characteristic information about the test system can be found in [24].

It is considered that a bulk PV energy generation system is integrated into bus number 6 on the reconfigurable MG for this short-term operational scheduling study. As put forth in Table 1, diesel DGs with 4 MW total maximum real power capacity operated at a unity power factor has been installed on different buses.

Table 1. The features of dispatchable DGs.

Dispatchable Units	Bus Number	Cost Function Coefficients of Dispatchable Units		
		a (£)	b (£/MW)	c (£/MW ²)
Diesel DG-1	14	25	87	0.0045
Diesel DG-2	18	28	92	0.0045
Diesel DG-3	32	26	81	0.0035

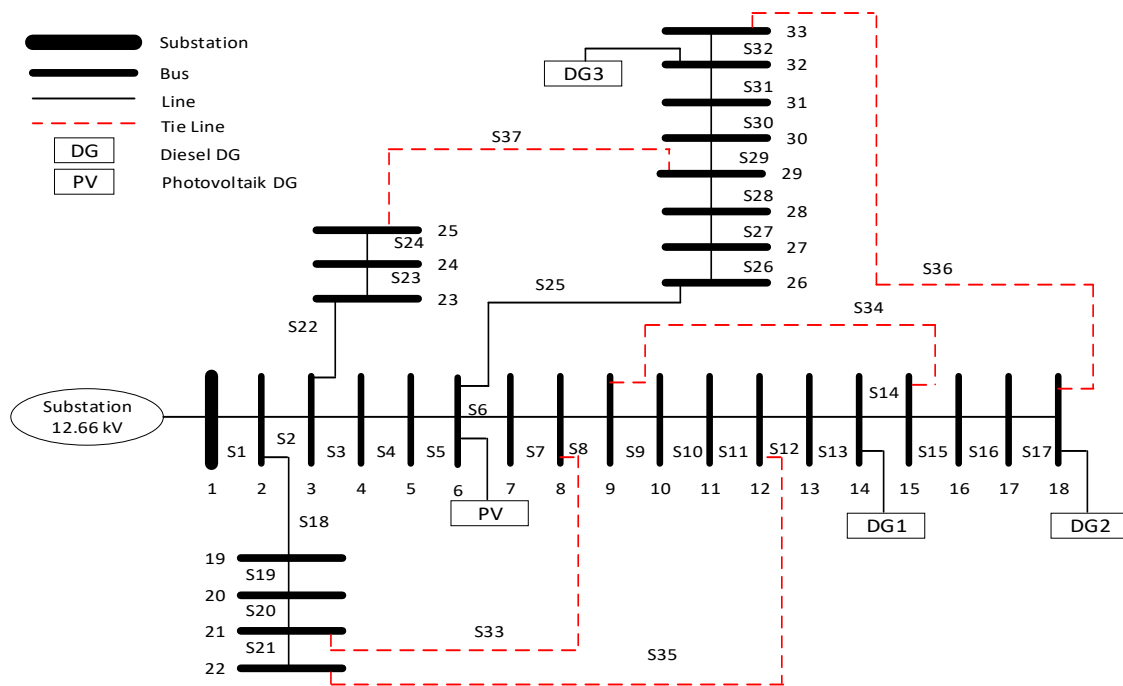


Figure 5. The standard 33-bus test system considered as a reconfigurable MG.

2.4. Forecasting Results for the Optimal Operational Scheduling Problem

The results in normalized and unnormalized data are reported in this section. The results measured on peak hours of each day instead of all 24 h are also reported. “N” and “U” denote the normalized and unnormalized data respectively. “P” denotes only peak-hour unnormalized data. Error calculating results for Load and PV power forecasting are presented in Tables 2 and 3 for the proposed RNN, Table 4 for the baseline FFNN, Table 5 for random guess results. Note that, MG optimal operational scheduling results are provided only when the forecast is performed on the last 20% of the days (from 08.01.2016 to 31.12.2016) with the proposed RNN, explicitly shown in Table 2.

Table 2. Power load and generation forecast errors with the proposed RNN tested only on the last 20% of the days (from 08.01.2016 to 31.12.2016).

Forecast Errors	Test Data	MAE	RMSE	MAPE	sMAPE	MASE
Power Demand	N	0.1361	0.2029	4.68%	4.68%	0.3778
	U	173.71	258.93	1.18%	1.19%	0.3778
	P	259.55	470.83	1.47%	1.49%	0.5361
PV Power Generation	N	0.2055	0.3861	14.96%	13.49%	0.9316
	U	77.74	146.06	14.00%	12.71%	0.9316
	P	216.59	269.83	25.53%	24.02%	0.8090

Table 3. Power load and generation forecast errors with the proposed RNN, 5-fold cross-validation results.

Forecast Errors	Test Data	MAE	RMSE	MAPE	sMAPE	MASE
Power Demand	N	0.1287 ± 0.0064	0.1850 ± 0.0115	5.59 ± 0.62%	5.45 ± 0.49%	0.3543 ± 0.0191
	U	164.20 ± 8.16	236.14 ± 14.72	1.21 ± 0.07%	1.21 ± 0.07%	0.3543 ± 0.0191
	P	195.36 ± 40.49	288.60 ± 103.75	1.19 ± 0.21%	1.20 ± 0.21%	0.3958 ± 0.0868
PV Power Generation	N	0.1984 ± 0.0076	0.3821 ± 0.0123	15.95 ± 1.34%	14.01 ± 0.86%	0.8990 ± 0.0408
	U	75.03 ± 2.88	144.54 ± 4.66	14.78 ± 1.15%	13.10 ± 0.75%	0.8990 ± 0.0408
	P	217.37 ± 9.85	273.29 ± 14.24	27.72 ± 2.65%	25.07 ± 1.16%	0.8165 ± 0.0483

Table 4. Power load and generation forecast errors with the baseline FFNN, 5-fold cross-validation results.

Forecast Errors	Test Data	MAE	RMSE	MAPE	sMAPE	MASE
Power Demand	N	0.1948 ± 0.0176	0.2788 ± 0.0672	8.61 ± 1.15%	8.50 ± 1.06%	0.5361 ± 0.0475
	U	248.57 ± 22.51	355.74 ± 85.76	1.84 ± 0.17%	1.84 ± 0.17%	0.5361 ± 0.0475
	P	334.22 ± 196.39	554.18 ± 557.28	1.62 ± 0.78%	1.67 ± 0.87%	0.6795 ± 0.4102
PV Power Generation	N	0.2549 ± 0.0166	0.4424 ± 0.0236	25.78 ± 4.11%	23.45 ± 3.79%	1.1549 ± 0.0764
	U	96.40 ± 6.28	167.35 ± 8.91	23.37 ± 3.51%	21.40 ± 3.29%	1.1549 ± 0.0764
	P	197.15 ± 26.09	276.35 ± 31.02	22.06 ± 5.47%	25.83 ± 6.83%	0.7401 ± 0.0977

Table 5. Power load and generation forecast errors with random guesses drawn from normal distribution $N(\mu(x), \sigma(x))$ where x is either power demand or PV generation, 5-fold cross-validation results (5 random repetitions).

Forecast Errors	Test Data	MAE	RMSE	MAPE	sMAPE	MASE
Power Demand	N	1.1429 ± 0.0400	1.4202 ± 0.0481	54.94 ± 6.80%	45.96 ± 2.79%	3.1462 ± 0.1179
	U	1458.44 ± 51.10	1812.26 ± 61.39	10.85 ± 0.59%	10.77 ± 0.42%	3.1462 ± 0.1179
	P	1512.44 ± 157.48	1881.04 ± 195.12	9.14 ± 0.46%	9.60 ± 0.61%	3.0625 ± 0.3595
PV Power Generation	N	1.1110 ± 0.0162	1.4167 ± 0.0210	177.92 ± 5.06%	105.62 ± 1.33%	5.0349 ± 0.1279
	U	420.22 ± 6.12	535.87 ± 7.96	155.78 ± 3.73%	100.44 ± 1.22%	5.0349 ± 0.1279
	P	673.60 ± 44.06	812.88 ± 44.89	68.83 ± 1.44%	94.98 ± 2.86%	2.5306 ± 0.1971

MAE and RMSE results of normalized data are similar in demand and PV power generation forecasting although MAPE and sMAPE errors are much higher in PV power generation. The fact that PV power generation values are much lower than demand values generating higher MAPE and sMAPE results can be indicated as the primary reason. Regarding overall forecasting results, the proposed RNN method shows much better performance comparing with the FFNN method in all cases. However, especially with the tested data which are only on the last 20% of the days (from 08.01.2016 to 31.12.2016), it shows best ever performance when unnormalized MAPE results are benchmarked. Also, random results are the worst of all these results although they are drawn from a normal distribution where the statistics of the data are encapsulated. Only for PV power generation peak hours, FFNN provides better MAE and MAPE metrics which is at the end a one-shot prediction instead of 24-h predictions. On the other hand; peak hour demand or generation values are more variable between different days, compared to 24-h predictions.

Furthermore, it can be seen when Table 6 is observed that more accurate forecasting results can be attained with the proposed DRNN Bi-LSTM model in comparison with other methods in the literature that are based on deep architecture, in both demand and PV generation forecasting frameworks over the short-term horizon. It provides the possibility for integrating renewable energy efficiently, reducing pollutant emissions, as well as keeping the stability of power system operation.

The forecasting results of aggregated electrical energy demand and the bulk PV generation on January 8, 2016 will be used as the given experimental setup in the optimal operational scheduling of the MG, thereby contributing to promoting interaction and supply-demand balance in the grid-connected reconfigurable MG [37]. The comparative chart of the demand forecasts and actual demand values are presented in Figure 6. Solar power output estimation results are given with actual solar power generation data in Figure 7, comparatively.

Table 6. Benchmarking the error rates with other deep structured methods in the literature.

Methods	Forecasting Interval	Forecasting Level	Benchmarking Methods	Data	Load Forecasting Test MAPE	PV Power Forecasting Test MAPE
Proposed approach (DRNN-BiLSTM)	24-h (1-h resolution)	Aggregated grid power load	-	01.01.2012–31.12.2016	1.18%	14.00%
D-CNN [72]	24-h (30 min resolution)	Aggregated grid power load	Extreme Learning Machine (ELM), RNN, CNN, ARIMA	From the last week of April 2018 till the second week of July 2018	2.15%	-
Copula-DBN [73]	24-h (1-h resolution)	Aggregated grid power load	Classical NNs, SVR, ELM, and DBN	During the year of 2016	5.25%	-
DRNN-LSTM [37]	24-h (1-h resolution)	Aggregated residential power load	MLP network and SVM	01.01.2018–01.02.2018	7.43%	15.87%
Parallel CNN-RNN [41]	24-h (1-h resolution)	Aggregated grid power load	LR, SVR, DNN, CNN-RNN	10.02.2000–31.12.2012	1.405%	-

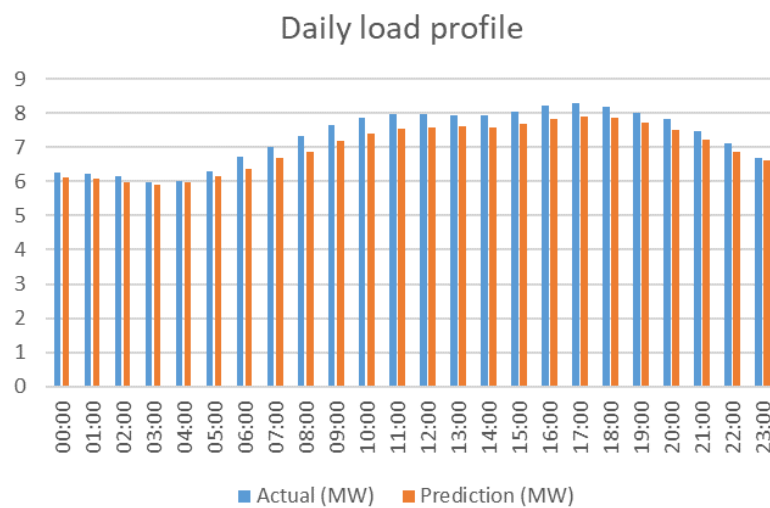


Figure 6. Day-ahead actual and predicted demand.

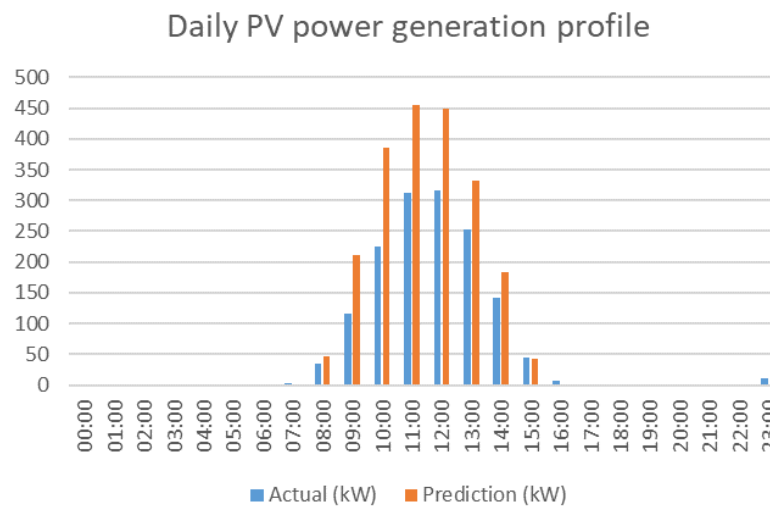


Figure 7. Day-ahead (24-h) actual and predicted PV power output.

2.5. PSO&SPSO Procedure for the Optimal Operational Scheduling Problem

The SPSO algorithm is used in this approach for determining the switch positions, whereas the OD of the DG units is performed with the basic PSO algorithm at each iteration. Both algorithms have a common objective function which is minimizing the real power loss of the whole system. In the whole PSO&SPSO algorithm, swarm population (n) is 50 and the maximum iteration number is 200. The convergence curve of the combined PSO&SPSO algorithm is presented in Figure 8 and here fitness denotes the best solution. The rest of the parameters' set values are the same as in [28].

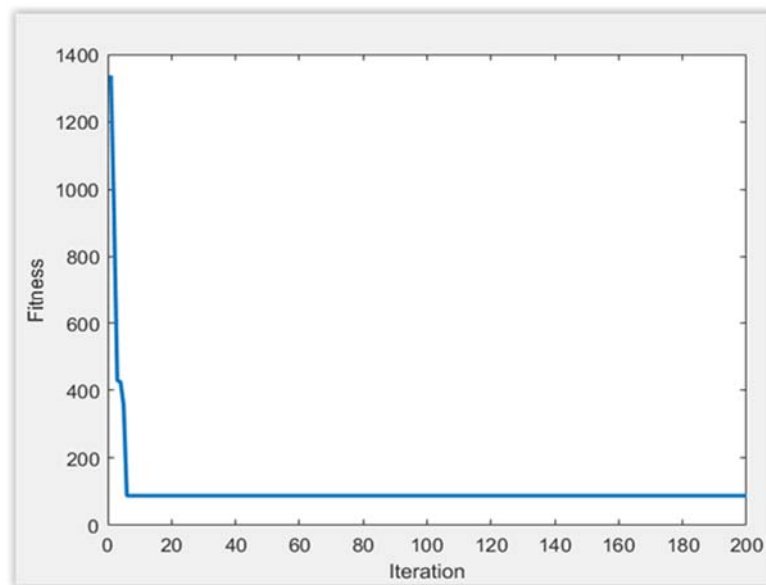


Figure 8. The convergence curve of the proposed algorithm.

The test reconfigurable MG system with all the specified sectionalizing switches and tie switches is presented in Figure 5. The dimension of the SPSO algorithm is equal to the number of loops formed when all tie switches in the reconfigurable MG are closed. Each dimension corresponds to a search space consisting of all the branches of the loop indicated with that dimension. There are five loops concerning the optimization problem in this reconfigurable MG test system once the tie switches (S33, S34, S35, S36, S37) are closed. Thus, the dimension is equal to five, and the search space in the SPSO algorithm is also represented by this dimension as five. The loops comprised of the respective branches (switches) on the reconfigurable MG test system are the same as in [24]. The connection in this case to the feeder must be maintained continuously, and the switches that are common in the loops should appear only in one loop at a time. The switches of the test system that are not in any loop do not belong to any of the search spaces and hence the optimization algorithm does not consider them. It should be examined whether the test system is radial or not once the switches are selected and the connection conditions are met [74]. The optimal solution can be assigned when the radiality condition is obtained.

2.6. The Optimal Operational Scheduling Problem Test Results

Five different case studies have been performed in this section with the results presented in the following tables. The proposed single-objective problem is optimized at every time sequence in all optimization case studies presented in this study by considering the forecasted and actual hourly load demand and non-dispatchable DG unit (PV) output power profiles of the test reconfigurable MG system which has all integrated DG units (Three diesel DGs & a solar generation unit). The power market price schedule is used as presented in [24] for the economic evaluation of the operational scheduling framework. The cases that are performed for the short-term (24-h) period are presented in short as follows:

- *Case I:* Basic AC load flow analysis is performed in this case to see the test total daily real power losses of the system without performing any operational study on the reconfigurable MG system.
- *Case II:* OD of dispatchable diesel DGs is realized here by using the conventional PSO algorithm to monitor the effects of these DGs on the test system within the day.
- *Case III:* NR algorithm is applied to the test system via the SPSO method for this case.
- *Case IV:* This is a sequential study of case II and case III. Namely, NR is performed following OD of diesel DGs.
- *Case V:* Finally, in this case, NR and OD of diesel DGs are performed simultaneously by using the combined approach of conventional and selective PSO algorithms to observe the effects of both optimal operation studies at the same time.

The estimated daily total load for the MG test system used is 168,407.5 kW and the estimated daily total solar power generation is 1467.74 kW. When the basic power flow (PF) analysis is performed in line with the first case, the daily total real power loss in the system is 17681 kW with the estimated data and it corresponds to 10.49% of the estimated total energy consumption. Furthermore, the daily average minimum voltage profile on the MG test system is about 0.96 p.u. Hourly estimated energy demand values and corresponding market pricing can be found in Figure 9. Accordingly, total daily energy cost is calculated as 14,283.16 Euro with estimated data by performing basic load flow analysis on the test reconfigurable MG system.

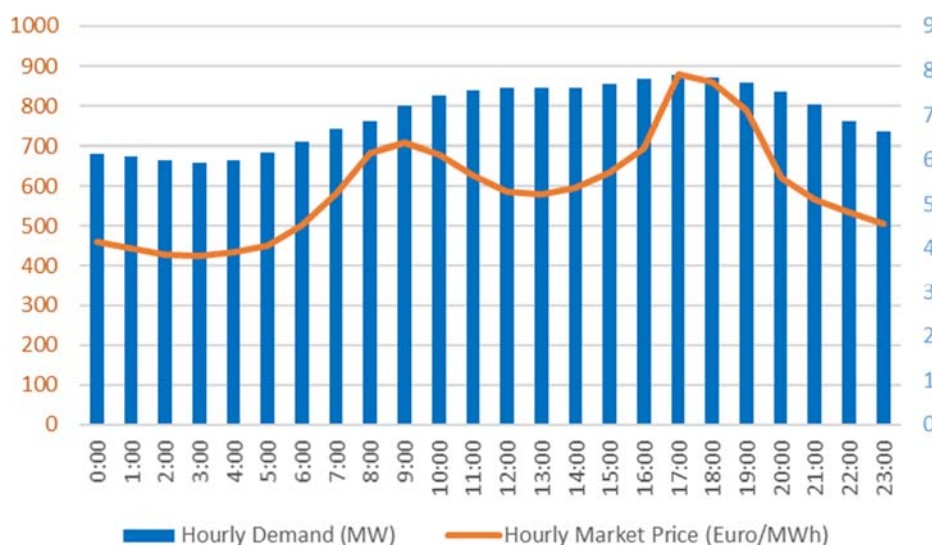


Figure 9. Hourly estimated demand and the hourly market price of the test reconfigurable MG system.

In case II, only OD of diesel DGs has performed on the test reconfigurable MG system with the estimation data and the daily total real power loss amount of 10,164 kW as seen in Table 7 which corresponds to 6.04% of the total estimated energy consumption. The average voltage level obtained by the PF study is 0.96 p.u. which has reached the level of 0.98 p.u. with the OD study as expected. With these results, total daily energy cost is calculated as 13,680.61 Euro. In the scope of the third case study, only NR framework is realized on the test system with the estimated data and it has been determined that the daily total real power loss amount is 9359 kW, which is equal to 5.56% of the total energy consumption. The contribution of the NR study to the voltage profile is observed when this study is performed with real data as seen in Table 7. When the energy cost amount is calculated with these results it corresponds to 14,288.19 Euro. It can be observed when these studies are compared through Table 7 that daily real power loss value with NR study is less than that of the OD study while the voltage profile of the OD study is better than the voltage profile of NR study.

Table 7. OD of diesel DG units and NR results.

Hour	Case II			P _L (kW)	V _{min} (p.u.)	Case III						
	Dispatch of DGs (MW)					Open Switches (Number)	P _L (kW)	V _{min} (p.u.)				
	DG1	DG2	DG3									
00:00	0.580	1.209	1.318	162	0.98	21	6	14	30	26	233	0.96
01:00	0.371	0.921	1.041	252	0.98	35	6	14	30	26	226	0.95
02:00	1.147	0.423	0.263	353	0.98	11	6	14	29	26	264	0.96
03:00	0.412	0.498	1.180	269	0.98	11	7	34	30	26	209	0.95
04:00	0.226	0.222	0.725	482	0.98	21	7	14	31	26	246	0.98
05:00	0.768	0.395	1.364	225	0.98	21	6	14	30	26	235	0.96
06:00	0.631	0.936	0.121	432	0.98	11	6	14	31	26	309	0.96
07:00	0.728	0.333	0.805	433	0.98	11	6	14	30	26	353	0.96
08:00	1.240	0.600	0.529	364	0.98	11	6	14	31	26	370	0.97
09:00	0.880	0.381	0.857	461	0.98	11	6	14	30	26	435	0.97
10:00	0.077	0.971	1.259	450	0.97	35	6	34	30	26	370	0.96
11:00	0.972	0.658	1.249	343	0.97	11	6	14	31	26	473	0.96
12:00	0.379	1.024	1.017	449	0.97	21	6	14	31	26	436	0.96
13:00	0.609	0.264	1.230	532	0.97	11	6	14	30	26	511	0.97
14:00	1.257	0.068	0.911	517	0.97	11	6	14	30	26	507	0.96
15:00	1.300	0.242	1.370	366	0.97	11	7	14	30	26	473	0.96
16:00	0.716	0.642	0.517	653	0.97	21	6	14	31	26	474	0.96
17:00	1.260	0.121	0.470	712	0.97	11	6	34	31	26	466	0.96
18:00	0.784	1.008	0.465	547	0.97	11	6	14	17	26	685	0.96
19:00	1.126	1.017	0.694	388	0.97	11	6	14	30	26	532	0.96
20:00	1.095	0.808	0.985	341	0.98	21	6	14	31	26	422	0.96
21:00	0.290	0.409	0.382	781	0.98	11	6	14	30	26	442	0.95
22:00	1.254	0.121	0.9505	370	0.98	11	6	14	31	26	370	0.96
23:00	0.244	1.000	1.332	282	0.98	11	7	14	30	26	318	0.95
				10,164	0.98						9359	0.96
				(Daily total)	(Daily avr.)						(Daily total)	(Daily avr.)

NR operation is actualized right after OD operation in case IV with estimated load data in this test system with the daily total real power loss amount determined as 8670 kW which corresponds to 5.15% of the total energy consumption. Furthermore, the average voltage profile has been improved to 0.97 p.u. and the total daily energy cost is calculated as 13,591.09 Euro. Thus, the lowest daily total real power loss and energy cost values have been obtained with this framework in comparison with the results of previous case studies.

It is important to notice that the results are very close to those of the NR study in terms of real power loss, while the energy cost result is quite parallel with the result OD of diesel DGs framework result as seen in Figures 10 and 11, respectively.

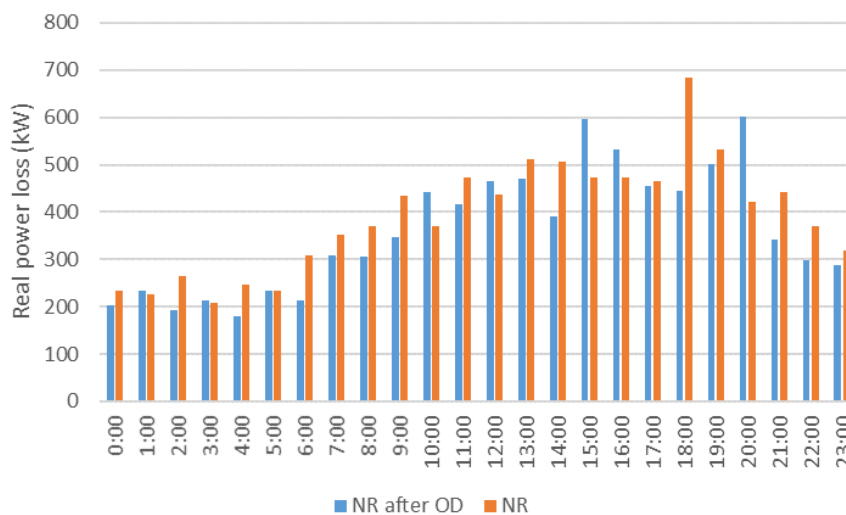


Figure 10. Daily real power loss comparative chart of case III and IV.

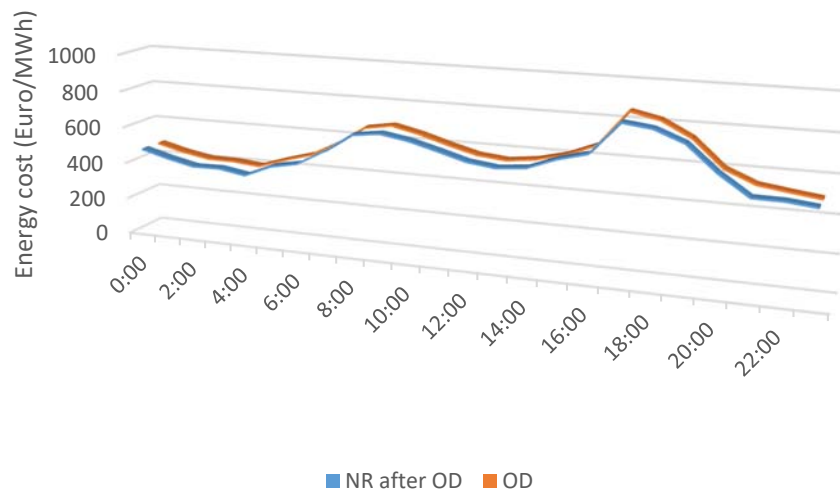


Figure 11. Daily energy cost comparative chart of case II and IV.

Consequently, NR and OD operations are performed simultaneously in case IV with the estimated load data where the daily real power loss amount is 7590 kW which corresponds to 4.51% of the total energy consumption in case 5. No improvement in the voltage profile is observed as can be seen in Table 8. However, it is still quite a good profile since it is close to the unit voltage level (1 p.u.). As a result of this case study, the lowest daily total real power loss and total energy cost amount of 13,526.1 Euro have been attained in comparison with the previous cases. The fourth case (NR after OD) has the closest results to this final case study in terms of real power loss and energy cost among all previous cases. It is worth observing the stacked chart of the daily real power loss curve for each case study since the curves of the last three studies that include NR operation are substantially parallel to each other as seen in Figure 12.

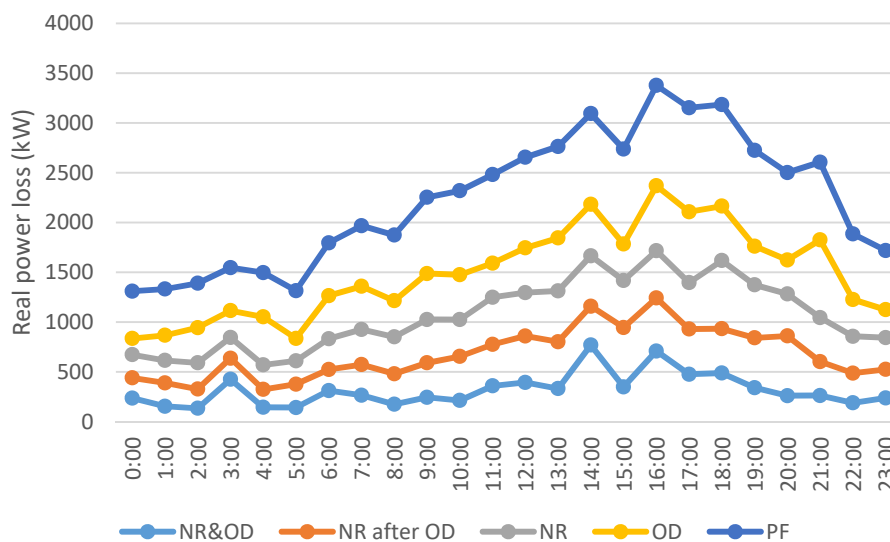


Figure 12. Daily real power loss chart of all cases.

Furthermore, the NR&OD results are calculated for every 20 days within the scope of case 5 to observe the status of each month and the differences between the actual and estimated values during the one-year test period are presented to put forth the overall impact of the forecasting method on short-term optimal operational scheduling framework in Figure 13. As can be seen from the graph, the two curves run parallel to each other or in other words, there is a very small difference between

the actual and the predicted values. Total daily active power loss is 13.31 MW in the NR&OD study obtained with the test values and 12.88 MW for the same study with the estimated values as can be seen in the following figure when the mean values for this test year are calculated for these 19 measurements. Moreover, MAPE is calculated as 10.11 with these measurements.

Table 8. Simultaneous application of NR and OD of diesel DGs’ results.

Hour	Open Switches (Number)	Dispatch of DGs (MW)			P _L (kW)	V _{min} (p.u.)
		DG1	DG2	DG3		
		00:00	11 6 13 29 25	0.405		
01:00	11 6 13 29 25	0.432	0.701	1.327	153	0.96
02:00	11 6 13 29 26	0.634	0.838	0.954	133	0.95
03:00	11 6 13 30 25	0.143	0.264	0.521	424	0.96
04:00	11 6 13 29 25	0.855	0.841	1.125	143	0.95
05:00	11 6 13 29 25	0.908	0.798	0.809	140	0.96
06:00	11 6 13 29 25	0.899	0.404	0.365	311	0.96
07:00	11 6 13 29 25	0.766	0.362	0.835	264	0.94
08:00	11 6 13 29 25	1.199	0.691	1.191	173	0.96
09:00	11 7 13 29 26	0.505	0.851	0.777	243	0.96
10:00	11 6 13 29 25	1.299	1.292	0.362	212	0.94
11:00	11 6 13 30 25	1.024	1.182	0.718	358	0.97
12:00	11 6 13 30 25	0.431	0.648	1.393	393	0.98
13:00	11 6 13 29 25	0.898	0.725	0.659	331	0.95
14:00	11 6 13 30 26	0.144	0.678	0.224	768	0.95
15:00	11 6 13 29 25	1.210	0.802	0.324	348	0.94
16:00	11 6 13 29 26	0.680	0.102	0.716	708	0.95
17:00	11 6 13 30 25	1.261	0.144	0.710	475	0.95
18:00	11 6 13 30 26	0.371	0.623	0.919	487	0.96
19:00	11 6 13 29 25	0.579	0.547	1.159	340	0.96
20:00	11 6 13 29 26	1.234	1.242	0.098	259	0.96
21:00	11 6 13 29 25	1.138	0.331	0.893	261	0.96
22:00	10 6 13 29 25	1.099	1.174	0.335	188	0.95
23:00	11 6 13 29 26	1.188	0.232	0.664	237	0.95
					7590	0.96
					(Daily total)	(Daily avr.)

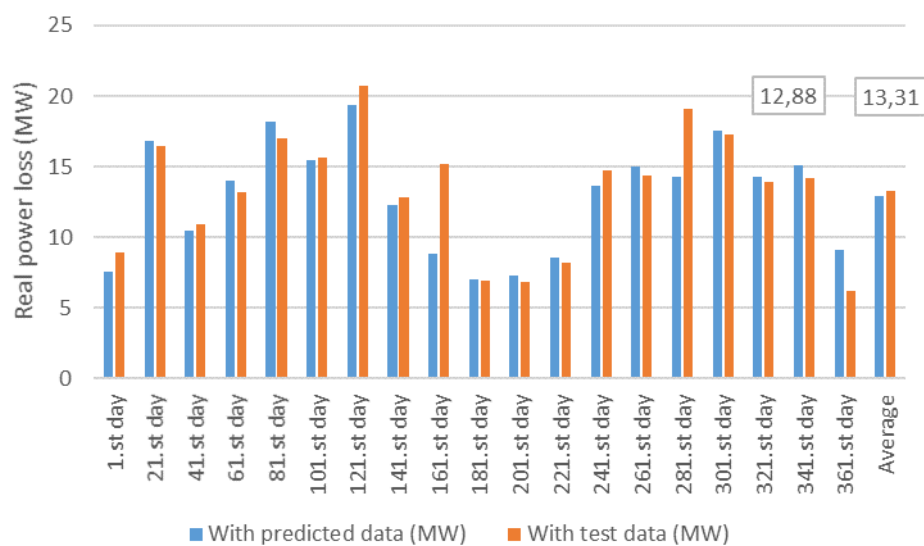


Figure 13. The daily total real power loss of every 20 days throughout the test year.

3. Conclusions

In this study, the time-varying nature of both the electrical load consumption and solar power output has been taken into account to support supply-demand balance within the scope of microgrid operational scheduling. To estimate aggregated power demand and the bulk PV output power over the short-term time period (day-ahead), a DRNN Bi-LSTM model has been proposed since conventional forecasting methods have limitations in modeling complex nonlinear problems and cannot take into consideration the time dependencies in the data set. Real-world datasets are used to test the DRNN Bi-LSTM model. They achieve excellent performance in forecasting aggregated power load and PV output power with MAPE values of 1.18% and 14%, respectively. These estimations are also performed by the FFNN method to observe the difference with traditional methods. The reason RNN mostly provides better results than the FFNN model lies behind the fact that the proposed model can learn long-term relationships between the sequential input data and the values to be predicted. Also, it has more learnable parameters compared to the FFNN model. In addition, the forecasting results put forth that the DRNN Bi-LSTM model performs better than the majority of the deep architected methods surveyed in the literature. Therefore, the proposed DRNN Bi-LSTM model presents the potential for making more accurate short-term forecasting for day-ahead optimal operational scheduling of reconfigurable MG. The value of daily total active power loss in the reconfigurable MG test system decreases by 56% within the scope of day-ahead optimal operational scheduling with the demand and PV power data while it reduces by 57% with the estimated demand and PV power data via simultaneous NR and OD of diesel DGs' framework. The difference between the real power loss percentages obtained via the actual and forecasted data with DRNN Bi-LSTM for operational scheduling study is very small as is the difference between forecasted demand and PV power with DRNN Bi-LSTM and the actual demand and PV power data. Therefore, the proposed DRNN Bi-LSTM model has the potential for providing more accurate short-term forecasting for day-ahead optimal operational scheduling of reconfigurable MG.

Nevertheless, there are still some studies that can improve this work. The forecasting and optimization algorithms are run separately here, and the dynamic mechanism between them will be studied in future work. Afterwards, a real-time application will be added for more dynamic results in a coordinated manner with this dynamic study. To achieve more precise forecast results, shorter time periods (30 sec., 15 sec.) will be utilized instead of hourly data for real-time application studies. Besides, optimal operational scheduling of the electrical energy storage units and demand response programs will be addressed to improve the resiliency of the microgrid. Finally, development of novel algorithms that can replace the developed algorithms will be studied for improving forecasting and optimal operational scheduling studies in microgrids.

Author Contributions: F.Y. and M.B.Y. designed the model, gathered the input data, executed the simulations, and accomplished writing of the paper. A.A.-M. and M.B. supervised the entire work and edited the language. All authors have read and agreed to the published version of the manuscript.

Funding: This research was funded partially by the HeatReFlex-Green and Flexible Heating/Cooling project, (www.heatreflex.et.aau.dk) funded by Danida Fellowship Centre and the Ministry of Foreign Affairs of Denmark under the grant no. 18-M06-AAU.

Conflicts of Interest: The authors declare no conflict of interest.

Nomenclature

$\mu(x)$	the mean value of feature x
$\sigma(x)$	the standard deviation
p_j	a prediction by the proposed model
a_j	the corresponding actual value
n	is the size of the test set
x	decision vector

dv	number of decision variables
$f(x)$	optimization problem's objective function
$h_i(x)$	equality constraint that should be satisfied
$g_i(x)$	inequality constraints that should be satisfied
p	number of equality constraint
q	number of inequality constraints
P_L	total active power losses of the network
I_i	the real component of the current at branch i
R_i	branch resistance
b	sets of branches
$Cost_{MG}$	purchasing energy cost from the main grid
$Cost_{DG}$	the energy production cost of dispatchable DGs
v^b	forecasted price of the purchasing energy
P^b	value of purchased energy
P_{DG}	the output power of a distributed DG unit
a, b, c	cost function coefficients of a dispatchable DG
P_{EP}	exchanged power between the MG and the upstream grid
P_{MGL}	power consumption of each load of MG
N_{MGL}	number of MG loads
N_{DG}	number of DGs
V_i	the voltage level of each bus
V_{min}	the minimum voltage level of each bus
V_{max}	the maximum voltage level of each bus
I_i	the flowing current amount on the i^{th} branch
I_i^{max}	thermal rating of the i^{th} branch
β_b	a binary variable that defines a branch status (0—open, 1—closed)
N_b	set of branches (b)
m	number of network buses
N_{sub}	number of substations
S_D	selective search space at each dimension D
T	total number of samples in the training data
Y_t	training samples
k	iteration number
ω_{max}	the initial inertia weight value
ω_{min}	the final inertia weight value
DN	number of selected positions in dimension D
v_{min}	the minimum velocity of each particle
v_{max}	the maximum velocity of each particle

References

1. Ahmad, A.; Javaid, N.; Mateen, A.; Awais, M.; Khan, Z.A. Short-Term load forecasting in smart grids: An intelligent modular approach. *Energies* **2019**, *12*, 164. [[CrossRef](#)]
2. Ng E., J.; El-Shatshat, R.A. Multi-microgrid control systems (MMCS). In Proceedings of the IEEE PES General Meeting, Providence, RI, USA, 25–29 July 2010; pp. 1–6. [[CrossRef](#)]
3. Anvari-Moghaddam, A.; Seifi, A.R. A comprehensive study on future smart grids: definitions, strategies and recommendations. *J. N. C. Acad. Sci.* **2011**, *127*, 28–34.
4. Huh, J.; Seo, K. Smart Grid Framework Test Bed Using OPNET and Power Line Communication. In Proceedings of the Joint 8th International Conference on Soft Computing and Intelligent Systems (SCIS) and 17th International Symposium on Advanced Intelligent Systems (ISIS), Hokkaido, Japan, 25–28 August 2016; pp. 736–742.
5. Huh, J.; Seo, K. Hybrid Advanced Metering Infrastructure Design for Micro Grid Using the Game Theory Model. *Int. J. Softw. Eng. Appl.* **2015**, *9*, 257–268. [[CrossRef](#)]

6. Evar C., U.; Milana, T. Operational scheduling of microgrids via parametric programming. *Appl. Energy* **2016**, *180*, 672–681.
7. Shi, W.; Xie, X.; Chu, C.; Gadh, R. Distributed Optimal Energy Management in Microgrids. *IEEE Trans. Smart Grid* **2015**, *6*, 1137–1146. [[CrossRef](#)]
8. Yu J., J.Q.; Hou, Y.; Lam, A.; Li, V. Intelligent Fault Detection Scheme for Microgrids with Wavelet-based Deep Neural Networks. *IEEE Trans. Smart Grid* **2017**, *10*, 1694–1703. [[CrossRef](#)]
9. Shariatzadeh, F.; Vellaithurai, C.B.; Biswas, S.S.; Zamora, R.; Srivastava, A.K. Real-time implementation of intelligent reconfiguration algorithm for Microgrid. *IEEE Trans. Sustain. Energy* **2014**, *5*, 598–607. [[CrossRef](#)]
10. Ma, J.; Ma, X. A review of forecasting algorithms and energy management strategies for microgrids. *Syst. Sci. Control. Eng.* **2018**, *6*, 237–248. [[CrossRef](#)]
11. Kusakana, K. Optimal scheduling for distributed hybrid system with pumped hydro storage. *Energy Convers. Manag.* **2016**, *111*, 253–260. [[CrossRef](#)]
12. Wan, C.; Zhao, J.; Song, Y.; Xu, Z.; Lin, J.; Hu, Z. Photovoltaic and solar power forecasting for smart grid energy management. *CSEE J. Power Energy Syst.* **2016**, *1*, 38–46. [[CrossRef](#)]
13. Anvari-Moghaddam, A. Global Warming Mitigation Using Smart Micro-Grids. In *Global Warming—Impacts and Futur Perspective*; Bharat, R.S., Ed.; IntechOpen: London, UK, 2012; Chapter 4, pp. 119–134. [[CrossRef](#)]
14. Rabiee, A.; Sadeghi, M.; Aghaeic, J.; Heidari, A. Optimal operation of microgrids through simultaneous scheduling of electrical vehicles and responsive loads considering wind and PV units uncertainties. *Renew. Sustain. Energy Rev.* **2016**, *57*, 721–739. [[CrossRef](#)]
15. Xiao, Z.; Li, T.; Huang, M.; Shi, J.; Yang, J.; Yu, J.; Wu, W. Hierarchical MAS Based Control Strategy for Microgrid. *Energies* **2010**, *3*, 1622–1638. [[CrossRef](#)]
16. Dimeas, A.L.; Hatziargyriou, N.D. A MAS architecture for microgrids control. In Proceedings of the 13th International Conference on Intelligent Systems Application to Power Systems, Arlington, VA, USA, 6–10 November 2005; pp. 402–406.
17. Kish, G.; Lee, J.; Lehn, P. Modelling and control of photovoltaic panels utilising the incremental conductance method for maximum power point tracking. *IET Renew. Power Gener.* **2012**, *6*, 259. [[CrossRef](#)]
18. Kim, J.C.; Huh, J.H.; Ko, J.S. Improvement of MPPT Control Performance Using Fuzzy Control and VGPI in the PV System for Micro Grid. *Sustainability* **2019**, *11*, 5891. [[CrossRef](#)]
19. Xu, Y.; Xie, L.; Singh, C. Optimal scheduling and operation of load aggregators with electric energy storage facing price and demand uncertainties. In Proceedings of the North American Power Symposium, Boston, MA, USA, 4–6 August 2011.
20. Anwar, T.; Sharma, B.; Chakraborty, K.; Sirohia, H. Introduction to Load Forecasting. *Int. J. Pure Appl. Math.* **2018**, *119*, 1527–1538.
21. Pires, A.J. Short-term load forecasting based on ANN applied to electrical distribution substations. In Proceedings of the 39th International Universities Power Engineering Conference, Bristol, UK, 6–8 September 2004; Volume 1, pp. 427–432.
22. Anvari-Moghaddam, A.; Seifi, A.R. Study of forecasting renewable energies in smart grids using linear predictive filters and neural networks. *IET Renew. Power Gener.* **2011**, *5*, 470–480. [[CrossRef](#)]
23. Anvari-Moghaddam, A.; Monsef, H.; Rahimi-Kian, A.; Nance, H. Feasibility study of a novel methodology for solar radiation prediction on an hourly time scale: A case study in Plymouth, United Kingdom. *J. Renew. Sustain. Energy* **2014**, *6*, 033107. [[CrossRef](#)]
24. Lee, E.; Shi, W.; Gadh, R.; Kim, W. Design and Implementation of a Microgrid Energy Management System. *Sustainability* **2016**, *8*, 1143. [[CrossRef](#)]
25. Alani, A.Y.; Osunmakinde, I.O. Short-Term Multiple Forecasting of Electric Energy Loads for Sustainable Demand Planning in Smart Grids for Smart Homes. *Sustainability* **2017**, *9*, 1972. [[CrossRef](#)]
26. Pal, S.; Sen, S.; Sengupta, S. Power network reconfiguration for congestion management and loss minimization using Genetic Algorithm. In Proceedings of the Michael Faraday IET International Summit, Kolkata, India, 12–13 September 2015; pp. 291–296.
27. Possemato, F.; Paschero, M.; Livi, L.; Rizzi, A.; Sadeghian, A. On the impact of topological properties of smart grids in power losses optimization problems. *Int. J. Electron. Power Energy Syst.* **2016**, *78*, 755–764. [[CrossRef](#)]
28. Yaprakdal, F.; Baysal, M.; Anvari-Moghaddam, A. Optimal operational scheduling of reconfigurable microgrids in presence of renewable energy sources. *Energies* **2019**, *12*, 1858. [[CrossRef](#)]

29. Rao, R.S.; Ravindra, K.; Satish, K.; Narasimham, S.V.L. Power loss minimization in distribution system using network reconfiguration in the presence of distributed generation. *IEEE Trans. Power Syst.* **2013**, *28*, 317–325. [[CrossRef](#)]
30. Dahalan, W.M.; Mokhlis, H.; Ahmad, R.; Abu Bakar, A.H.; Musirin, I. Simultaneous Network Reconfiguration and DG Sizing Using Evolutionary Programming and Genetic Algorithm to Minimize Power Losses. *Arab. J. Sci. Eng.* **2014**, *39*, 6327–6338. [[CrossRef](#)]
31. Imran, A.M.; Kowsalya, M.; Kothari, D. A novel integration technique for optimal network reconfiguration and distributed generation placement in power distribution networks. *Int. J. Electron. Power Energy Syst.* **2014**, *63*, 461–472. [[CrossRef](#)]
32. Nguyen, T.T.; Truong, A.V.; Phung, T.A. A novel method based on adaptive cuckoo search for optimal network reconfiguration and distributed generation allocation in distribution network. *Int. J. Electron. Power Energy Syst.* **2016**, *78*, 801–815. [[CrossRef](#)]
33. Jiang, H.; Ding, F.; Zhang, Y. Short-term load forecasting based automatic distribution network reconfiguration. In Proceedings of the 2017 IEEE Power & Energy Society General Meeting, Chicago, IL, USA, 16–20 July 2017; pp. 1–5.
34. Gu, Y.; Jiang, H.; Zhang, J.J.; Zhang, Y.; Muljadi, E.; Solis, F. Load forecasting based distribution system network reconfiguration—A distributed data-driven approach. In Proceedings of the 2017 51st Asilomar Conference on Signals, Systems, and Computers, Pacific Grove, CA, USA, 29 October–1 November 2017; pp. 1358–1362.
35. Selvaraj, K.R.; Sundararaj, S.; Ravi, T. Artificial Neural Network Based Load Forecasting and Economic Dispatch with Particle Swarm Optimization. *Int. J. Sci. Eng. Res.* **2013**, *4*, 139–145.
36. Arif, M.; Liu, Y.; Haq, I.U.; Ashfaq, A. Load forecasting using neural network integrated with economic dispatch problem. *Int. J. Electron. Comput. Eng.* **2018**, *12*, 900–905.
37. Wen, L.; Zhou, K.; Yang, S.; Lu, X. Optimal load dispatch of community microgrid with deep learning based solar power and load forecasting. *Energy* **2019**, *171*, 1053–1065. [[CrossRef](#)]
38. Wu, X.; Cao, W.-H.; Wang, D.; Ding, M. A Multi-Objective Optimization Dispatch Method for Microgrid Energy Management Considering the Power Loss of Converters. *Energies* **2019**, *12*, 2160. [[CrossRef](#)]
39. Gutiérrez-Alcaraz, G.; Galvan, E.; Cabrera, N.G.; Javadi, M. Renewable energy resources short-term scheduling and dynamic network reconfiguration for sustainable energy consumption. *Renew. Sustain. Energy Rev.* **2015**, *52*, 256–264. [[CrossRef](#)]
40. Xu, Y.; Xie, L.; Singh, C. Optimal scheduling and operation of load aggregator with electric energy storage in power markets. In Proceedings of the North American Power Symposium, Boston, MA, USA, 4–6 August 2011.
41. He, W. Load Forecasting via Deep Neural Networks. *Procedia Comput. Sci.* **2017**, *122*, 308–314. [[CrossRef](#)]
42. Zheng, J.; Xu, C.; Zhang, Z.; Li, X. Electric load forecasting in smart grids using Long-Short-Term-Memory based Recurrent Neural Network. In Proceedings of the 2017 51st Annual Conference on Information Sciences and Systems (CISS), Baltimore, MD, USA, 22–24 March 2017; pp. 1–6.
43. Bouktif, S.; Fiaz, A.; Ouni, A.; Serhani, M.A. Optimal Deep Learning LSTM Model for Electric Load Forecasting using Feature Selection and Genetic Algorithm: Comparison with Machine Learning Approaches. *Energies* **2018**, *11*, 1636. [[CrossRef](#)]
44. Abdel-Nasser, M.; Mahmoud, K. Accurate photovoltaic power forecasting models using deep LSTM-RNN. *Neural Comput. Appl.* **2017**, *31*, 2727–2740. [[CrossRef](#)]
45. Chattopadhyay, D. Operational Planning of Power System: An Integrated Approach. *Energy Sources* **1994**, *16*, 59–73. [[CrossRef](#)]
46. Logenthiran, T.; Srinivasan, D. Short term generation scheduling of a Microgrid. In Proceedings of the TENCON 2009 - 2009 IEEE Region 10 Conference, Singapore, 23–26 November 2009; pp. 1–6.
47. Zhao, B.; Shi, Y.; Dong, X.; Luan, W.; Bornemann, J. Short-Term Operation Scheduling in Renewable-Powered Microgrids: A Duality-Based Approach. *IEEE Trans. Sustain. Energy* **2014**, *5*, 209–217. [[CrossRef](#)]
48. Yoon, A.-Y.; Moon, H.-J.; Moon, S.-I. Very short-term load forecasting based on a pattern ratio in an office building. *Int. J. Smart Grid Clean Energy* **2016**, *5*, 94–99. [[CrossRef](#)]
49. Jain, A.; Satish, B. Integrated approach for short term load forecasting using SVM and ANN. In Proceedings of the TENCON 2008—2008 IEEE Region 10 Conference, Hyderabad, India, 19–21 November 2008; pp. 1–6.

50. Hernandez, L.; Baladrón, C.; Aguiar, J.M.; Carro, B.; Sanchez-Esguevillas, A.J.; Lloret, J.; Massana, J.; Hernández-Callejo, L. A Survey on Electric Power Demand Forecasting: Future Trends in Smart Grids, Microgrids and Smart Buildings. *IEEE Commun. Surv. Tutor.* **2014**, *16*, 1460–1495. [[CrossRef](#)]
51. Hernández-Callejo, L.; Baladrón, C.; Aguiar, J.M.; Calavia, L.; Carro, B.; Sánchez-Esguevillas, A.; Sanjuan, J.; Gonzalez, A.; Lloret, J. Improved Short-Term Load Forecasting Based on Two-Stage Predictions with Artificial Neural Networks in a Microgrid Environment. *Energies* **2013**, *6*, 4489–4507. [[CrossRef](#)]
52. Chen, J.-F.; Wang, W.-M.; Huang, C.-M. Analysis of an adaptive time-series autoregressive moving-average (ARMA) model for short-term load forecasting. *Electron. Power Syst. Res.* **1995**, *34*, 187–196. [[CrossRef](#)]
53. Velasco, L.C.P.; Lou, D.; Paolo, G.; Bryan, M.B.f. Load Forecasting using Autoregressive Integrated Moving Average and Artificial Neural Network. *Int. J. Adv. Comput. Sci. Appl.* **2018**, *9*, 23–29. [[CrossRef](#)]
54. Saber, A.Y.; Alam, A.K.M.R. Short term load forecasting using multiple linear regression for big data. 2017 IEEE Symposium Series on Computational Intelligence (SSCI), Honolulu, HI, USA, 27 November–1 December 2017; pp. 1–6.
55. El-Hawary, M.; Mbamalu, G. Short-term power system load forecasting using the iteratively reweighted least squares algorithm. *Electron. Power Syst. Res.* **1990**, *19*, 11–22. [[CrossRef](#)]
56. Hernández-Callejo, L.; Baladrón, C.; Aguiar, J.M.; Calavia, L.; Carro, B.; Sánchez-Esguevillas, A.; Pérez, F.; Fernández, A.; Lloret, J. Artificial Neural Network for Short-Term Load Forecasting in Distribution Systems. *Energies* **2014**, *7*, 1576–1598. [[CrossRef](#)]
57. Moon, J.; Kim, Y.; Son, M.; Hwang, E. Hybrid Short-Term Load Forecasting Scheme Using Random Forest and Multilayer Perceptron. *Energies* **2018**, *11*, 3283. [[CrossRef](#)]
58. Chowdhury, D.; Sarkar, M.; Haider, M.Z.; Alam, T. Zone Wise Hourly Load Prediction Using Regression Decision Tree Model. In Proceedings of the 2018 International Conference on Innovation in Engineering and Technology (ICIET), Dhaka, Bangladesh, 25–27 October 2018; pp. 1–6.
59. Li, W.; Yang, X.; Li, H.; Su, L. Hybrid Forecasting Approach Based on GRNN Neural Network and SVR Machine for Electricity Demand Forecasting. *Energies* **2017**, *10*, 44. [[CrossRef](#)]
60. Mujeeb, S.; Javaid, N. Deep Long Short-Term Memory: A New Price and Load Forecasting Scheme for Big Data in Smart Cities. *Sustainability* **2019**, *11*, 987.
61. Gao, M.; Li, J.; Hong, F.; Long, D. Day-ahead power forecasting in a large-scale photovoltaic plant based on weather classification using LSTM. *Energy* **2019**, *187*, 115838. [[CrossRef](#)]
62. Wang, K.; Qi, X.; Liu, H. A comparison of day-ahead photovoltaic power forecasting models based on deep learning neural network. *Appl. Energy* **2019**, *251*, 113315. [[CrossRef](#)]
63. Gensler, A.; Henze, J.; Sick, B.; Raabe, N. Deep Learning for solar power forecasting—An approach using AutoEncoder and LSTM Neural Networks. In Proceedings of the 2016 IEEE International Conference on Systems, Man, and Cybernetics (SMC), Budapest, Hungary, 9–12 October 2016.
64. Alzahrani, A.; Shamsi, P.; Dagli, C.; Ferdowsi, M. Solar Irradiance Forecasting Using Deep Neural Networks. *Procedia Comput. Sci.* **2017**, *114*, 304–313. [[CrossRef](#)]
65. Dong, X.; Qian, L.; Huang, L. Short-term load forecasting in smart grid: A combined CNN and K-means clustering approach. In Proceedings of the 2017 IEEE International Conference on Big Data and Smart Computing (BigComp), Jeju Island, Korea, 13–16 February 2017; pp. 119–125.
66. Tian, C.; Ma, J.; Zhang, C.; Zhan, P. A Deep Neural Network Model for Short-Term Load Forecast Based on Long Short-Term Memory Network and Convolutional Neural Network. *Energies* **2018**, *11*, 3493. [[CrossRef](#)]
67. Zeng, P.; Li, H.; He, H.; Li, S. Dynamic Energy Management of a Microgrid Using Approximate Dynamic Programming and Deep Recurrent Neural Network Learning. *IEEE Trans. Smart Grid* **2019**, *10*, 4435–4445. [[CrossRef](#)]
68. Makridakis, S. Accuracy measures: theoretical and practical concerns. *Int. J. Forecast* **1993**, *9*, 527–529. [[CrossRef](#)]
69. Ben Hamida, I.; Salah, S.B.; Msahli, F.; Mimouni, M.F.; Msahli, F.; Mimouni, M.F. Optimal network reconfiguration and renewable DG integration considering time sequence variation in load and DGs. *Renew. Energy* **2018**, *121*, 66–80. [[CrossRef](#)]
70. Esmaeili, S.; Anvari-Moghaddam, A.; Jadid, S.; Guerrero, J.M. Optimal simultaneous day-ahead scheduling and hourly reconfiguration of distribution systems considering responsive loads. *Int. J. Electron. Power Energy Syst.* **2019**, *104*, 537–548. [[CrossRef](#)]

71. Hemmati, M.; Mohammadi-ivatloo, B.; Ghasemzadeh, S.; Reihani, E. Electrical power and energy systems risk-based optimal scheduling of reconfigurable smart renewable energy based microgrids. *Electron. Power Energy Syst.* **2018**, *101*, 415–428. [[CrossRef](#)]
72. Khan, S.; Javaid, N.; Chand, A.; Khan, A.B.M.; Rashid, F.; Afridi, I.U. Electricity Load Forecasting for Each Day of Week Using Deep CNN. *Adv. Intell. Syst. Comput.* **2019**, *927*, 1107–1119.
73. Ouyang, T.; He, Y.; Li, H.; Sun, Z.; Baek, S. Modeling and Forecasting Short-Term Power Load With Copula Model and Deep Belief Network. *IEEE Trans. Emerg. Top. Comput. Intell.* **2019**, *3*, 127–136. [[CrossRef](#)]
74. Golshannavaz, S.; Afsharnia, S.; Aminifar, F. Smart Distribution Grid: Optimal Day-Ahead Scheduling With Reconfigurable Topology. *IEEE Trans. Smart Grid* **2014**, *5*, 2402–2411. [[CrossRef](#)]



© 2020 by the authors. Licensee MDPI, Basel, Switzerland. This article is an open access article distributed under the terms and conditions of the Creative Commons Attribution (CC BY) license (<http://creativecommons.org/licenses/by/4.0/>).